

NRELAP5 PREDICTIONS OF KAIST HIGH PRESSURE CONDENSATION DATA USING EXISTING AND EXTENDED SHAH CONDENSATION CORRELATION

Pravin Sawant, John Marking, and Claudio Delfino

NuScale Power LLC

1100 NE Circle Blvd., Suite 200, Corvallis, OR 97330

psawant@nuscalepower.com; jmarking@ nuscalepower.com; cdelfino@ nuscalepower.com

ABSTRACT

NuScale Power LLC (NuScale) has commercially dedicated RELAP5-3D© [1], developed by the Idaho National Laboratory, as part of the safety analysis evaluation model. Development of the dedicated version of RELAP5-3D© for NuScale's reactor Design Certification Application will continue with an in-house proprietary version, NRELAP5. In the NuScale Small Modular Reactor (SMR) condensation plays an important role in the operation of passive safety systems. A Decay Heat Removal System (DHRS) in the NuScale SMR removes heat from the secondary side of the Steam Generator (SG) by natural circulation and condensation of steam. Condensation heat transfer in the NuScale containment vessel is critical to removing the heat from the reactor pressure vessel during various postulated accidents and transients. The pressure in these systems can reach high levels during their operation. For example, the DHRS pressure can increase to above 70 bar.

Condensation has been studied extensively under low pressure (i.e., near atmospheric pressure) conditions, and a significant amount of experimental data is available on the measurement of condensation heat transfer coefficients under low pressure conditions. However, experimental data at high pressure conditions is rare. Consequently, the NRELAP5 condensation heat transfer correlations need to be assessed for their applicability to high pressure condensation phenomena. In this paper, the NRELAP5 condensation heat transfer correlations are compared against the KAIST high pressure steam condensation data [2-3]. It was found that the existing NRELAP5 condensation heat transfer correlations under-predicted the condensation heat transfer rates measured in the KAIST experiments.

Shah recently published an improved version of his non-dimensional condensation correlation, which is identified as the extended Shah correlation for prediction of condensation in tube geometries [4]. The comparison against the KAIST experimental data showed that this correlation predicted the majority of the data within the measurement uncertainty. Therefore, the existing condensation heat transfer correlation in NRELAP5 was replaced by the extended Shah correlation. With this change, significant improvement is shown in NRELAP5's ability to predict the KAIST experimental data.

KEYWORDS

NRELAP5, RELAP5-3D, Small Modular Reactor, Decay Heat Removal System, Condensation, Shah Condensation Correlation

1. INTRODUCTION

1.1 Decay Heat Removal System in NuScale Reactor

A NuScale Power Module (NPM) (Figure 1) is an SMR with a power rating of 50 MWe (gross, 160 MWt). It is cooled by natural convection, with the pressurizer, SG, hot leg riser, downcomer (cold leg)

and core integrated into the reactor pressure vessel. A steel containment vessel envelops the reactor pressure vessel. The containment vessel is evacuated of air (vacuum) during power operation and is capable of withstanding high pressures during accident conditions. The NPM is submerged in a pool of water. The reactor building cooling pool is a stainless steel-lined concrete pool shared by all of the operating modules. Each module is covered by an individual concrete biological shield, and all of the modules and pool are enclosed in a single confinement building.

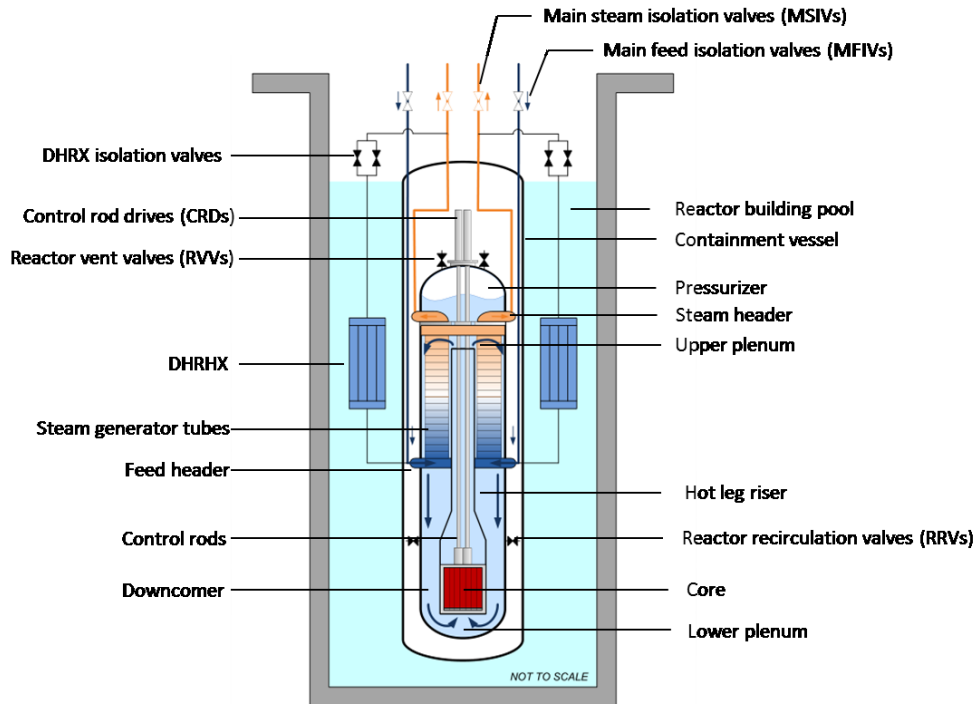


Figure 1. NuScale Power Module.

The NPM design includes passive safety systems and incorporates all primary system components within the reactor vessel. Use of passive safety systems for decay heat removal, emergency core cooling, and containment cooling eliminates safety-related external power requirements under accident conditions. NuScale modules and spent fuel pool are all located below grade and housed in controlled-access buildings.

DHRS is a passive system that transfers decay heat from the reactor to the reactor pool via the steam generators. It has two independent trains, each sized to handle full decay heat load. The decay heat removal heat exchangers (DHRHX) are vertical condenser tubes submerged in the reactor pool. The inlet to the DHRHX is connected to the main steam line. Opening of the valves at the inlet of the DHRHX actuates the system in conjunction with closing of the Main Feed and the Main Steam Isolation Valves. Steam is routed into the DHRX where it condenses and is returned back to the steam generator feedwater line in a closed loop mode of operation. After actuation, the DHRS pressure and temperature initially increase, and then decrease over time as energy is transferred to the reactor building pool. The DHRS pressure can increase above 70 bar during the transients.

1.2 KAIST High Pressure Condensation Data

Steam condensation inside a tube has been studied extensively and there is substantial information available throughout the scientific literature. However, one aspect that is not as well supported by data is

the performance of a condenser tube under high pressure steam. Reference [2] represents a PhD thesis that addressed this aspect as it has become increasingly relevant in the nuclear industry. The experiments in Reference [2] were performed at KAIST (Korea Advanced Institute of Science and Technology) to study steam condensation phenomena under high pressure in relatively large diameter tubes which are used in passive heat removal components of advanced nuclear reactors, including the NuScale DHRHX.

Table I summarizes the details of the test section used in the KAIST experiments. A schematic of the experimental facility is shown in Figure 2 [2, 3]. The major components of the test facility include: steam generator which supplied steam (maximum power 200 kW), test section tube, the cooling pool (cools the test section), steam line (transports steam from steam generator to the test section inlet), condensate drain line, lower plenum (or condensate collection tank) and air supply system. The test section was immersed in the cooling pool and was cooled by boiling and/or single-phase convective heat transfer on the outside surface of the test section.

Table I. KAIST Test Section Geometry

Parameter	Description/Value
Geometry	Single circular cross-section tube
Inside diameter, ID (cm)	4.62
Outside diameter, OD (cm)	5.08
Wall thickness, δ (mm)	2.3
Active length, L (m)	1.8
Material	Stainless steel 316

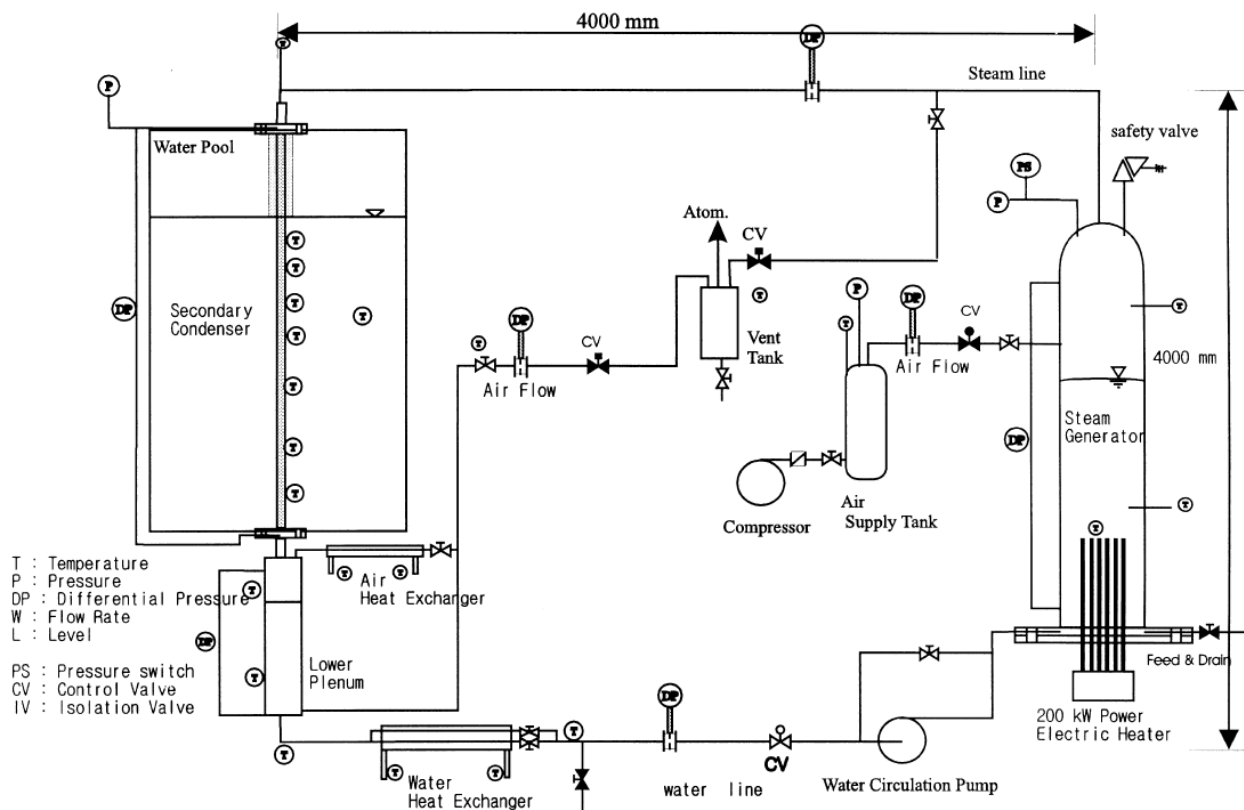


Figure 2. Schematic of KAIST Experiment [2, 3].

The test section was a vertical tube with an inside diameter of 4.62 cm and an effective heat transfer length of 1.8 m. The thickness of the tube wall was 2.3 mm. To reduce the entrance effect, the top 0.5 m length of the test section was insulated. The test section was submerged in the cooling pool of width 1.2 m \times 1.2 m and 2.5 m height. A steam line with an inside diameter 2.34 cm was connected from the top of the steam generator to the top of the test section. The condensate from the test section was drained to the lower plenum (or condensate collection tank) by gravity and then pumped back to the steam generator. More details of the test section geometry are available in References [2] and [3].

K-type thermocouples with a 1 mm outer diameter were used to measure the temperatures at the center of the test section (bulk steam temperature), on the inside and outside surfaces of the test section, and in the cooling pool. Bulk steam temperature at the center of the test section was measured at 4 elevations (0, 50, 100 and 170 cm from test section inlet) using sheathed ungrounded thermocouples. Test section outer surface temperature was measured at seven (7) elevations (2, 10, 35, 70, 90, 135, and 165 cm from test section inlet) using ungrounded thermocouples. Test section inner surface temperature was measured at ten (10) elevations (2, 10, 20, 35, 50, 70, 90, 110, 135, and 165 cm from the test section inlet) using 12 the grounded thermocouples. Absolute test pressure, test section pressure drop, inlet steam flow rate, and condensate flow rate were also measured. A 64 channel Hewlett Packard Data Acquisition System with maximum sampling rate of 100 kHz was used to acquire the measurements from all experimental instrumentation including: 45 thermocouples, 3 absolute pressure transducers, and 8 differential transducers. Further details on measurements and instrument specifications can be found in References [2] and [3].

The experiments were started by purging all non-condensable gas (i.e., air) from the test loop. This was done by supplying steam to the test loop and venting it to the atmosphere through the vent valve located below the test section. After all non-condensable gas was purged, the vent valve was closed and the test section was allowed fill with the condensate by keeping the condensate drain valve closed. After the test section was completely filled, steam generator pressure was increased to the test pressure. As soon as the test pressure was reached, the condensate drain valve was opened and the condensate recirculation pump was started. A constant water level in the lower plenum was maintained by control of the recirculation pump flow rate. Data acquisition was started after the process had reached a steady state. The experiments were also performed to study the effect of non-condensable gases. However, these experiments are not considered in the current study. Fifty one (51) experiments (344 data points) with pressure ranging from 0.794 MPa to 7.3 MPa were conducted using pure steam. Since the KAIST experiments were not performed under the NQA-1 2008/2009a program [5], the experimental data was first qualified following the guidance provided by NQA-1 2008/2009a, Part III, Subpart 3.3, Nonmandatory Appendix 3.1 "Guidance on Qualification of Existing Data". The data from fifteen (15) tests covering a pressure range of 1.071 to 7.305 MPa was qualified and selected for the assessment in this report. Table II shows the pressure and inlet steam mass flow rate for the selected data sets. These data sets account for total 109 data points.

Reference [2] provided a detailed analysis of the uncertainties in the measurements of test section inside wall surface temperatures, heat transfer coefficient, and mass flow. In the KAIST experiments, the heat flux across the tube wall was calculated from the measurement of inside and outside tube wall surface temperatures. Since the thickness of the test section tube wall is very small (2.3 mm), the measured heat flux is very sensitive to the error in placement or locations of the thermocouples. The uncertainty in the local heat transfer coefficient was calculated using an error propagation method. The analysis accounted for the uncertainty in the measurement of inner wall temperature (6%), outer wall temperature (2%), bulk steam temperature (1.5%), wall conductivity (2.5%), and wall mean radius (3%). The uncertainty in measurement of condensation heat transfer coefficient was estimated to be 28.2%.

Table II. KAIST Data Sets Selected for the Current Study

Experiment ID	Pressure (MPa)	Inlet Steam Mass Flow (kg/s)
25010802	1.071	0.0290
1501101	1.479	0.0401
1401101	1.749	0.0444
9050101	2.100	0.0481
27030501	2.621	0.0510
25010805	3.045	0.0436
27030502	3.490	0.0610
17010202	4.053	0.0477
27030801	4.559	0.0736
27030704	5.260	0.0735
27030602	5.316	0.0524
27030702	6.021	0.0890
27030703	6.656	0.0869
27030701	7.155	0.0883
26030503	7.305	0.1041

1.3 Condensation Correlations in RELAP5 3-D and NRELAP5

The condensation model in RELAP5-3D© and NRELAP5 Version Beta-0 was based on use of the Nusselt formulation for laminar regime [6] and the 1979 Shah correlation [7] for turbulent regime. The condensation heat transfer coefficient is calculated as the maximum of the Nusselt and Shah correlations.

Shah presented the following empirical condensation correlation in 1979 [7] based on wide range of experimental data:

$$h_{TP}/h_{LS} = 1 + 3.8/Z^{0.95} \quad (1)$$

where h_{TP} is condensation heat transfer coefficient and h_{LS} is the heat transfer coefficient of the liquid phase flowing alone and is given by following equation:

$$h_{LS} = 0.023 \left(\frac{k_f}{D} \right) Re_{LS}^{0.8} Pr_f^{0.4} \quad (2)$$

and

$$Z = \left(\frac{1}{x} - 1 \right)^{0.8} P_r^{0.4} \quad (3)$$

- Re_{LS} Reynolds number calculated assuming liquid phase flowing alone
- Pr_f Prandtl number of the liquid
- P_r Reduced pressure
- x vapor flow quality
- k_f thermal conductivity of liquid
- D tube diameter

NRELAP5 Version 1.0 implemented the extended Shah condensation heat transfer correlation published in 2009 [4]. This correlation provides an additional correction term that depends on the viscosity of the liquid (μ_f) and vapor (μ_g). This is defined as:

$$h_l = h_{LS}(1 + 3.8/Z^{0.95}) \left(\frac{\mu_f}{14\mu_g} \right)^n \quad (4)$$

$$n = 0.0058 + 0.557P_r \quad (5)$$

More importantly, the extended Shah formulation includes three regions: a turbulent region, a transition region, and a laminar region. Equation (4) for h_l is used for the condensation heat transfer coefficient in turbulent region. In the transition region, the h_l is summed to the Nusselt heat transfer coefficient (h_{nu}) which is used for the laminar region. Shah suggested the use of following Nusselt laminar heat transfer coefficient:

$$h_{nu} = 1.32Re_{LS}^{-1/3} \left[\frac{\rho_f(\rho_f - \rho_g)gk_f^3}{\mu_f^2} \right]^{1/3} \quad (6)$$

A dimensionless superficial vapor velocity parameter (J_g^*) is used to map the three condensation regions:

$$J_g^* = \frac{xG}{(gD\rho_g(\rho_f - \rho_g))^{0.5}} \quad (7)$$

Where,

G = Total mass flux

g = gravitational constant

ρ_g = Density of liquid phase

ρ_f = Density of gas phase

The condensation heat transfer Region I (i.e., turbulent region) occurs when

$$J_g^* \geq 1/(2.4Z + 0.73) \quad (8)$$

The condensation heat transfer Region III (i.e., laminar region) occurs when

$$J_g^* \leq 0.89 - 0.93 \exp(-0.087 \times Z^{-1.17}) \quad (9)$$

The condensation heat transfer coefficient in Region I (turbulent region) is given by Equation (4), h_l . In the transition region (Region II), the heat transfer coefficient is sum of Equations (4) and (6), $h_l + h_{nu}$. In the laminar region (Region III), the heat transfer coefficient is given by Equation (6), h_{nu} .

The extended Shah correlation has been assessed against the extensive data that includes tube diameters from 2 to 49 mm, reduced pressure from 0.0008 to 0.9, inlet flow rate from 4 to 820 kg/m²s, and all liquid Reynolds number from 68 to 85000.

2. NRELAP5 MODEL

The NRELAP5 model of the KAIST experimental facility is significantly simplified with respect to the facility. The input model consists of a single pipe to represent the condenser with a series of boundary conditions to reflect the fluid and material conditions. Figure 3 shows the simplified model. The condenser tube is represented by a one-dimensional PIPE element (PIPE-140) constructed with eight axial nodes. Two Time-Dependent Volume (TDVs) components represent the inlet (TDV-995) and outlet (TDV-997) boundary conditions. Mass flow into the condenser is driven via a Time-Dependent Junction

3. RESULTS

Figure 4 shows comparison of condensation heat transfer coefficient, inside wall temperature, and liquid film flow rate as a function of axial position between the NRELAP5 and RELAP5-3D calculated results and the measured data for experiment with Test ID 27030703. Similar comparison is shown for experiment with Test ID 27030801 in Figure 5. RELAP5-3D with the Nusselt correlation for the laminar regime, 1979 Shah correlation for turbulent regime, and the maximum of the Nusselt and 1979 Shah correlations for the transition regime under-predicted the condensation heat transfer coefficient. As observed from Figures 4 and 5, significant improvements in the predictions are obtained using the extended Shah correlation in NRELAP5 Version 1.0.

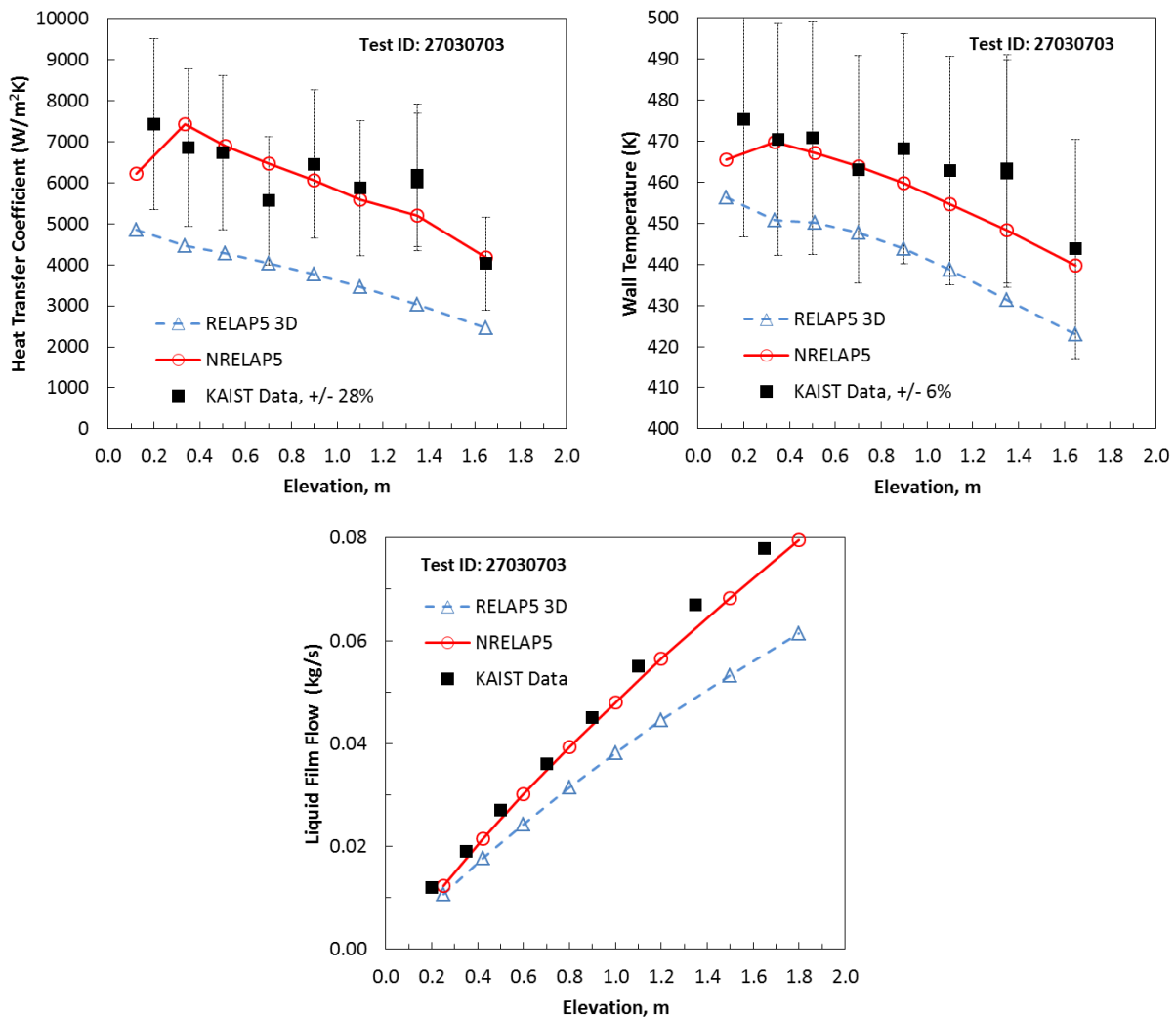


Figure 4. Comparison of KAIST Data vs NRELAP5 Heat Transfer Coefficient (P = 66.6 bar).

As described in Section 1.3, the extended Shah correlation uses the Nusselt correlation (Eq. 6) for the laminar regime and the modified Shah condensation correlation (Eq. 4) for turbulent regime. The transition regime condensation heat transfer coefficient in the extended Shah correlation is calculated by summing the Nusselt and the modified Shah condensation correlations instead of taking the maximum of these two correlations. The implementation of the extended Shah correlation results in a calculated heat transfer coefficient that is generally within the experimental uncertainty as indicated by the error bars (+/-

28%) in the figures. Most of the experimental data was predicted to be in the transition regime by the extended Shah correlation. As shown in Figures 4 and 5, the use of the extended Shah correlation also improved the calculated predictions of the test section inside wall surface temperatures and the liquid film mass flow rates. Similar results were obtained for all fifteen experiments (15) considered in this study.

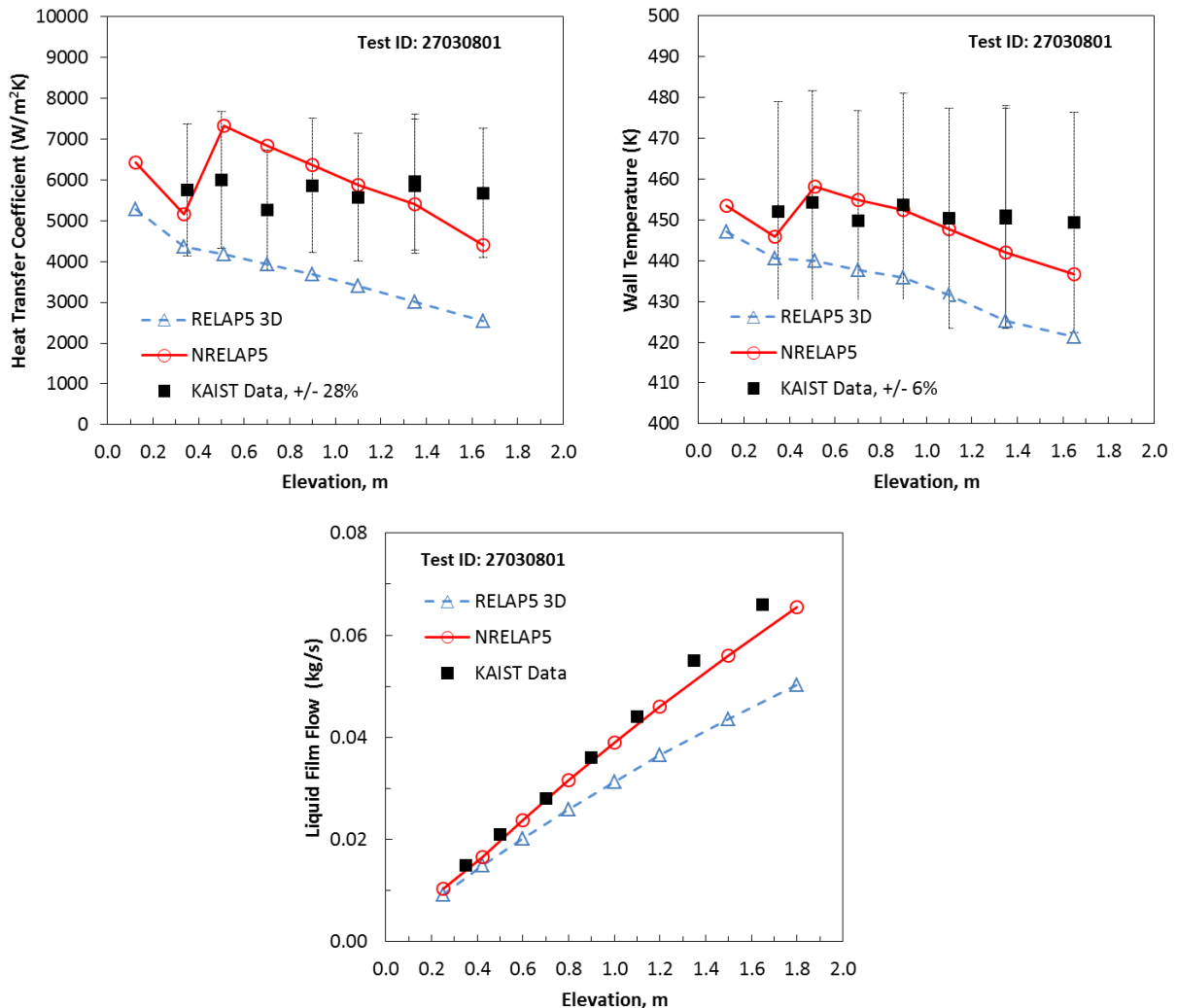


Figure 5. Comparison of KAIST Data vs NRELAP5 Heat Transfer Coefficient (P = 45.6 bar).

Figure 6 presents a summary of the measured versus predicted condensation heat transfer coefficients for all fifteen (15) KAIST test experiments considered in this study. With the use of extended Shah correlation, almost all of the NRELAP5 predictions lie within the experimental uncertainty.

3. CONCLUSIONS

The assessment of NRELAP5 against the KAIST high pressure condensation data showed that the existing condensation correlation in RELAP5-3D under-predicted the experimental data. The most recent extended Shah correlation was implemented in NRELAP5. The use of the extended Shah correlation in NRELAP5 significantly improved the predicted results. The comparisons presented in this paper show reasonable to excellent agreement between the calculated NRELAP5 results and the KAIST measured

experimental data for condensation heat transfer coefficients, wall temperature, and liquid film mass flow rate over a wide range of high pressure conditions.

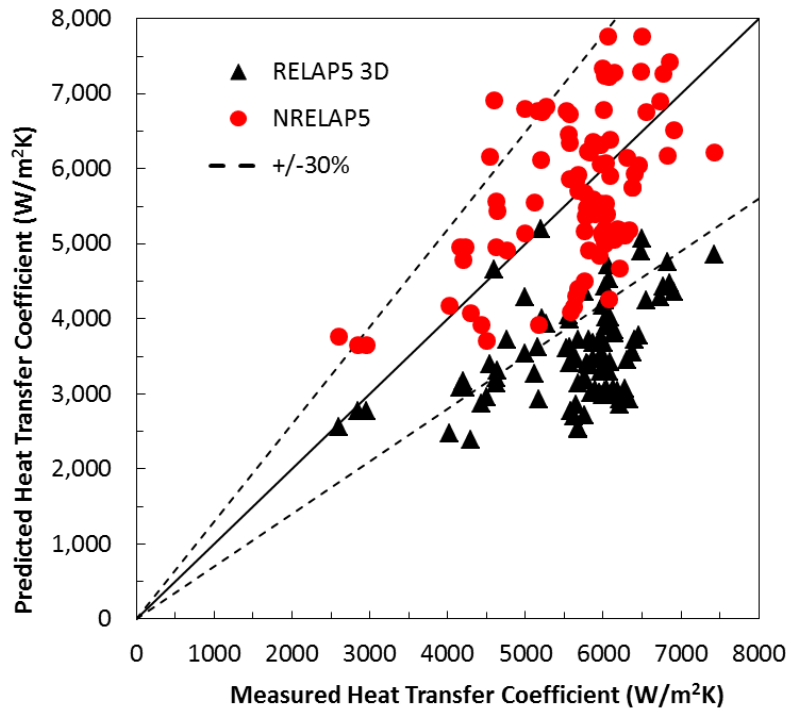


Figure 6. Measured vs Predicted Heat Transfer Coefficient.

REFERENCES

1. D. Prelewicz, B. Wolf, and C. Delfino, "Commercial Grade Dedication of RELAP5-3D©," 16th International Topical Meeting on Nuclear Reactor Thermal Hydraulics, August 30-September 4, 2015, Chicago, Illinois, USA.
2. S.J. Kim, "Turbulent Film Condensation of High Pressure Steam in a Vertical Tube of Passive Secondary Condensation System," Ph.D. Thesis, Department of Nuclear Engineering, Korea Advanced Institute of Science and Technology, February 2000.
3. S.J. Kim and H.C. No, "Turbulent Film Condensation of High Pressure Steam in a Vertical Tube", *Int. J. of Heat and Mass Transfer*, **43**, pp. 4031-4042 (2000).
4. M.M. Shah, "An Improved and Extended General Correlation for Heat Transfer during Condensation in Plain Tubes," *HVAC&R Research*, **15**(5), pp. 889-913 (2009).
5. American Society of Mechanical Engineers, Quality Assurance Requirements for Nuclear Facility Applications (QA), ASME NQA-1-2008 and addenda ASME NQA-1a-2009, New York, NY., NONMANDATORY APPENDIX 3.1, Guidance on Qualification of Existing Data.
6. W. Nusselt, "Die Oberflächenkondensation des Wasserdampfes," *Zeitschrift Ver. Deutsch. Ing.*, **60**, 1916, pp. 541-546 and 569-575.
7. M.M. Shah, "A General Correlation for Heat Transfer during Film Condensation in Tubes," *Int. J. of Heat and Mass Transfer*, **22**(4), pp. 547-556 (1979).
8. A.P. Colburn and O. A. Hougen, "Design of Cooler Condensers for Mixtures of Vapors with Noncondensing Gases," *Industrial and Engineering Chemistry*, **26**, pp. 1178-1182 (1934).
9. M.M. Shah, "Heat Transfer during Film Condensation in Tubes and Annuli: A Review of the Literature," *ASHRAE Transactions*, **87**(1), pp. 1086-1105 (1981).